ACOUSTIC IMAGING OF SPARSE SOURCES WITH ORTHOGONAL MATCHING PURSUIT AND CLUSTERING OF BASIS VECTORS

Trond F. Bergh[†,⋆] *Ines Hafizovic*[⋆] *Sverre Holm*[†]

[†] Department of Informatics, University of Oslo, Norway
[⋆] Squarehead Technology, Oslo, Norway

ABSTRACT

We have devised a greedy method for finding solutions to the sparse Deconvolution Approach for the Mapping of Acoustic Sources inverse problem using a variant of Orthogonal Matching Pursuit. The algorithm has two stages, wherein the first stage consists of selecting a subset of the basis vectors iteratively via a regularized inverse of the point spread function, and the second stage consists of constructing point source solutions using this basis subset and its coefficients via hierarchical agglomerative clustering. We have evaluated the algorithm on both synthetic and real data, and show that the overall accuracy in terms of direction of arrival and reconstructed source power is better than four other state of the art methods.

***Index Terms*—** Acoustic imaging, deconvolution, DAMAS, orthogonal matching pursuit, array processing.

1. INTRODUCTION

Acoustic imaging with microphone arrays has become the standard method for determining the magnitude and location of acoustic sources. The usual way of imaging with microphone arrays is conventional beamforming, also known as delay-and-sum (DAS) beamforming. However, as with any imaging device, the finite aperture of the microphone array limits the resolution of the resulting image (or source map). The result is a blurred image (or dirty source map), thus making it hard to distinguish sources in close proximity to each other. Beside the blurring of the main source image, the PSF further contaminates the source map with repeated weaker images of a source due to the sidelobes. These effects may be represented as a clean source map being convolved with a variable kernel, which is referred to as the point spread function (PSF). The PSF is essentially the impulse response of the imaging system. The process of cleaning up the source map by removing the array response is thus frequently referred to as deconvolution.

In [1] the authors define the deconvolution problem as a matrix inversion problem, and solve it iteratively with the Gauss-Seidel method, a procedure that was named the Deconvolution Approach for the Mapping of Acoustic Sources (DAMAS). The original formulation of DAMAS converges slowly, however, and by assuming a constant PSF over the imaging region, the DAMAS2/3 [2] methods solve the DAMAS problem faster in the Fourier domain [3].

A popular alternative to DAMAS is the original CLEAN (by appearance an acronym, but we have been unable to determine its meaning) method [4], originally developed for application in astrophotography. CLEAN and its derivatives [5, 6] form a family of algorithms for iteratively building up a "clean" source map (that is, without the polluting effect of the array response) from the "dirty" delay-and-sum image.

By assuming a small number of sources (sparse signal) relative to the number of points in the imaging grid the Sparsity Constrained-DAMAS (SC-DAMAS) [7] method solves the inverse problem using the Least Absolute Shrinkage and Selection Operator (LASSO) method [8]. Sarradj [9] uses eigendecomposition of the cross spectral matrix (CSM) into noise- and signal-subspaces to estimate source levels and positions. Suzuki [10] decomposes the CSM in a similar manner and uses a generalized inverse to find the source distribution with minimal ℓ_1-norm that best fits the largest eigenmodes of the CSM, a method that is referred to as Generalized Inverse Beamforming (GIB). Zhong et al. [11] seek a solution to the DAMAS inverse problem using basis pursuit denoising, which optimizes the sparsity of the solution. Chu et al. [12, 13] minimize an ℓ_2 cost function over both the source map and noise estimate simultaneously with a sparsity constraint on the source map.

Many of the above methods employ constrained convex optimization to solve the (sparse) DAMAS inverse problem. For sufficiently sparse signals a more efficient, though sub-optimal, approach is to use greedy algorithms [14]. Wang and Wu [15] apply a modified Orthogonal Matching Pursuit (OMP) [16] algorithm with a local search step to the Direction of Arrival (DOA) problem. Padois and Berry [17] use OMP to solve the standard DAMAS problem. In this paper we will present a sparse reconstruction algorithm for the standard DAMAS inverse problem using a regularized inverse, similar to Enhanced OMP (E-OMP) [18], with a subsequent clean-up step. The proposed method retains the speed of a greedy method while simultaneously giving greater accuracy in source positions and powers.

2. BACKGROUND THEORY

We model the sound field as a set of L monopole acoustic sources at positions $\{\vec{x}_l\}_{1\leq l\leq L}$ with complex source amplitudes as a function of frequency ω at a reference distance r_0 given by $S(\omega) \in \mathbb{C}^{L\times 1}$. The complex amplitudes at the microphone array can be written

$$X(\omega) = G(\omega)S(\omega) \in \mathbb{C}^{M\times 1}. \tag{1}$$

$G \in \mathbb{C}^{M\times L}$ is the propagation matrix whose elements can be expressed as $G_{m,l} = \frac{r_0}{||\vec{x}_m - \vec{x}_l||}\mathrm{e}^{-\mathrm{j}\omega\Delta_{m,l}}$, where $\vec{x}_{m/l}$ is the position of microphone m and source point l respectively, $\Delta_{m,l}$ is the propagation delay between the two, and c is the speed of sound.

The cross spectral matrix is given by $R(\omega) = X(\omega)X^H(\omega)$. In practice the CSM must be estimated from a finite number of samples which are usually split into K segments. The CSM is then estimated by averaging over the K short-time estimates. The imaging region is a set of points $\{\vec{x}_n\}_{1\leq n\leq N}$ in a regular rectangular grid. An acoustic image is a set of DAS power values for the imaging grid points, or scan points. The DAS power value for a single grid point may be written as (dropping the explicit frequency dependence from now on) $Y_n = \frac{1}{M^2} w_n^H R w_n$, where $w_n \in \mathbb{C}^{M\times 1}$ is the steering vector for grid point n whose elements are given by $(w_n)_m = \frac{||\vec{x}_n - \vec{x}_m||}{r_0} e^{-\mathrm{j}\omega\Delta_{m,n}}$.

Substituting the expressions for R and X into the expression for Y_n yields

$$Y_n = \frac{1}{M^2}\sum_{i=1}^{L}\sum_{j=1}^{L}\Big[w_n^H G_i G_j^H w_n \times \frac{1}{K}\sum_{k=1}^{K} S_{i,k}S_{j,k}^*\Big], \quad (2)$$

where G_i denotes column i of G and $S_{i,k}$ is the complex source amplitude of source i in the time segment k. Equation (2) can be written as a matrix equation by stacking the indices i and j, $Y = \tilde{A}\tilde{Q}$, where $\tilde{A} \in \mathbb{C}^{N\times L^2}$, and $\tilde{Q} \in \mathbb{C}^{L^2\times 1}$ is the vectorization of the source covariance matrix. The model sources are commonly assumed to be statistically independent, thus for sufficiently large K the cross terms $i \neq j$ in equation (2) approach zero and the expression for Y reduces to

$$Y = AQ, \quad (3)$$

where $A \in \mathbb{R}_{0+}^{N\times L}$ is the PSF for the scan points and $Q \in \mathbb{R}_{0+}^{L\times 1}$ is the source power vector. Eq. (3) is what we refer to as the DAMAS inverse problem [1].

The column set of A forms an overcomplete basis (or frame) for some subset of $\mathbb{R}^N$, with expansion coefficients for Y given by Q. Each column of A thus represents a single basis vector corresponding to a source grid point. If the positions of the actual sources do not coincide with modelled source grid the basis is said to be mismatched. In practical applications basis mismatch, noise, and finite sampling period usually mean that eq. (3) cannot be solved exactly, but instead one focuses on minimizing the residual $\rho = Y - AQ$.

Orthogonal Matching Pursuit (OMP) [16] is a procedure for iteratively generating a k-sparse approximation that minimizes the norm of the residual for a given measurement vector and basis by greedy choice of the support set for the solution vector. In OMP a single index is added to the support set in each iteration, thus the number of iterations should be equal to the sparsity of the source vector. The selected index is the one corresponding to the basis vector with the largest absolute inner product with the residual. All elements of the solution vector selected so far is updated in every iteration by an orthogonal projection of the measurement vector onto the space spanned by the selected basis vectors. This ensures that an index is never selected twice, and thus the number of iterations is bounded by the size of the basis set.

3. PROPOSED ALGORITHM

We propose a two-stage algorithm for finding solutions to the sparse DAMAS inverse problem, which we will refer to as Clustered OMP-DAMAS, or COMP-DAMAS for short. The first stage is listed in alg. 1, and is an iterative procedure similar to OMP ($[\,\cdot\,]_\Gamma$ denotes the submatrix/vector formed by the columns/elements indexed by Γ). The purpose of this step is to select a sparse subset of the basis vectors, given by the columns of A, to approximate the DAS image. Instead of choosing the basis vector with the largest absolute inner product with the measurement vector, we select the index of the largest absolute value of $\tilde{q} \in \mathbb{R}^L$ given by

$$\tilde{q} = \arg\min_q \left|\left|\rho^{(i-1)} - Aq\right|\right|_2 \approx A^\dagger \rho^{(i-1)}, \quad (4)$$

$$A^\dagger = \left(A^H A + \lambda\sigma_{\max}(A)\mathbb{1}_L\right)^{-1} A^H, \quad (5)$$

Algorithm 1 COMP-DAMAS 1st stage

Initialization:
$Q^{(0)} \leftarrow 0$ {Preliminary solution/expansion coefficients}
$\Gamma^{(0)} \leftarrow \emptyset$ {Support set}
$\rho^{(0)} \leftarrow Y$ {Residual}
for $s = 1$ **to** L **do**
  $\tilde{k} = \arg\max_k \left|(A^\dagger \rho^{(s-1)})_k\right|$
  $\Gamma^{(s)} \leftarrow \Gamma^{(s-1)} \cup \tilde{k}$
  $Q^{(s)} \leftarrow (A^H_{\Gamma^{(s)}} A_{\Gamma^{(s)}})^{-1} A^H_{\Gamma^{(s)}} Y$
  $\rho^{(s)} \leftarrow Y - A_{\Gamma^{(s)}} Q^{(s)}$
  if $\left(\left|\left|\rho^{(s-1)}\right|\right|_2 - \left|\left|\rho^{(s)}\right|\right|_2\right) / \left|\left|\rho^{(s-1)}\right|\right|_2 \leq \delta$ **then**
    Exit loop
  end if
end for

i.e. the largest absolute regularized least-squares coefficient of the residual ρ. This is a regularized version of the selection rule used in E-OMP [18], but unlike E-OMP we only select a single index in each iteration, and instead of backtracking we employ a clean-up step which is detailed later. $A^\dagger$, given by eq. (5), is a Moore-Penrose inverse with an added regularization term with parameter λ. $\sigma_{\max}(\,\cdot\,)$ denotes the largest singular value of the argument and $\mathbb{1}_L$ the identity matrix of size $L \times L$. The regularization is necessary in all problems of practical interest (otherwise we would have a closed form solution of eq. (3)). In another departure from OMP, we allow the support set to grow beyond the number of sources, N_s (which is assumed known), and terminate the loop when the relative change in the norm of the residual is smaller than the parameter δ. Further additions to the support set will have small coefficients and thus not substantially improve the approximation $Y \approx A_\Gamma Q_\Gamma$, i.e. the remaining residual is assumed to be noise dominated. Regularized inverse reconstruction is chosen because it tends to produce a large, but relevant support set. Inner product reconstruction on the other hand tends to introduce noise into the support set as soon as the set size exceeds the number of sources.

The approximation of Y from stage 1, $A_\Gamma Q_\Gamma$, is a linear combination of a subset of the columns of A, thus Q_Γ may in general have negative coefficients. Since the elements of Q in eq. (3) represent source powers, the final source vector estimate must be non-negative. Additionally, a real point source may have been represented by more than one basis vector. In the second stage of the algorithm we thus seek to combine the basis vectors and coefficients from stage 1 in such a way that negative coefficients are eliminated (by being combined with basis vectors with positive coefficients) and each real source is represented by a single basis vector. The first step of stage 2 is to group the basis vectors by hierarchical bottom-up (agglomerative) clustering using the degree of overlap of the normalized beampatterns of two grid points as a measure of distance. This choice of the distance measure is motivated by the heuristic argument that two basis vectors are more likely to represent a single source if the degree of overlap is high. In particular, the distance function used in the clustering is the inverted symmetric PSF, given by

$$d_{i,j} = 1 - \frac{1}{2}\left(\frac{\left|w^H(\vec{x}_i)g(\vec{x}_j)\right|^2}{\left|w^H(\vec{x}_j)g(\vec{x}_j)\right|^2} + \frac{\left|w^H(\vec{x}_j)g(\vec{x}_i)\right|^2}{\left|w^H(\vec{x}_i)g(\vec{x}_i)\right|^2}\right), \quad (6)$$

where $\vec{x}_{i/j}$ denotes the positions of a pair of grid points. The distances between clusters are updated at each step by averaging the values of $d_{i,j}$ for all members of a cluster. The clustering procedure is halted when there are N_s clusters, or when the minimal distance between any two clusters exceeds a parameter $0 < \gamma < 1$. In practice a value of $\gamma = 0.85$ seems to provide a good balance between including too many basis vectors and including too few.

After the clustering operation the chosen index set is partitioned into $N_c \geq N_s$ disjoint sets $\Gamma = \Gamma_1 \cup \Gamma_2 \cup \ldots \cup \Gamma_{N_c}$. As each cluster of basis vectors, indexed by Γ_n, and their associated coefficients Q_{Γ_n}, is hypothesized to represent a single source, we seek to find an index $k_n \in \{1, \ldots, L\}$ and a single coefficient $\hat{Q}_{k_n} > 0$ that minimizes $\left|\left| A_{k_n} \hat{Q}_{k_n} - A_{\Gamma_n} Q_{\Gamma_n} \right|\right|_2$. The solution is

$$k_n = \arg\min_k \left|\left| A_k - \frac{A_{\Gamma_n} Q_{\Gamma_n}}{\sum_{i \in \Gamma_n} Q_i} \right|\right|, \tag{7}$$

$$\hat{Q}_{k_n} = (A_{k_n}^H A_{k_n})^{-1} A_{k_n}^H A_{\Gamma_n} Q_{\Gamma_n}. \tag{8}$$

The values of k_n and $\hat{Q}_{k_n}$ for each cluster define the N_c-sparse approximate solution to the DAMAS inverse problem, eq. (3).

4. EVALUATION ON SYNTHETIC DATA

To evaluate the accuracy of the proposed algorithm we have simulated the acoustic field of three different source configurations with varying levels of noise. Noise is modelled as additive Gaussian i.i.d. at each receiver. The simulated sources emit uncorrelated white noise and are located in a plane parallel to the array at a distance of 4.3 m. The imaging grid consists of 20×15 source points. Scenario 1 consists of three separated sources with power 1. Scenario 2 consists of two sources with powers 0.7 and 1.0, separated by an angle of $14.6°$. Scenario 3 consists of four separated sources with powers 0.25, 0.50, 0.75 and 1.0 in a square pattern. The first scenario is a general test case, the second scenario is intended to test the ability to separate closely spaced sources, and the third scenario tests the dynamic range. The three scenarios have been simulated with signal-to-noise ratios of ∞, 0 dB, -6 dB, -9 dB, and -12 dB (relative to a source at a distance of 4.3 m with power 1). The simulated microphone array has 16×16 elements in a regular rectangular grid and an aperture of 39 cm $\times$ 39 cm.

We have applied COMP-DAMAS, as well as four other deconvolution methods to the delay-and-sum (DAS) images to estimate the actual source strengths and positions. The DAS image is formed from $K = 100$ snapshots of 128 samples each at a frequency $f = 2$ kHz. The reference methods used are OMP-DAMAS [17], CLEAN-SC [6], SC-RDAMAS [12, 13] and GIB [10]. An example of the deconvolved images resulting from application of the five algorithms to the DAS image is shown in fig. 1.

To quantify the fidelity of the reconstructed acoustic images we use the average position error, measured in meters, and the average relative source power error. The average position error is defined as the distance between the actual source position and the center of the pixel with the largest power in its vicinity in the reconstructed image, averaged over all sources. The minimal attainable position error is thus limited by the resolution of the imaging grid. The average relative power error is defined as the absolute difference between the actual source power and the reconstructed source power, relative to the actual source power, averaged over all sources. The results for all simulated source scenarios and noise conditions are listed in tables 1 and 2. The stars behind the numbers for CLEAN-SC mean that the algorithm failed to separate the two sources and produced a single strong source. The daggers behind the numbers for GIB signify that the algorithm failed to identify the weakest source, and that the average was taken over the 3 strongest sources.

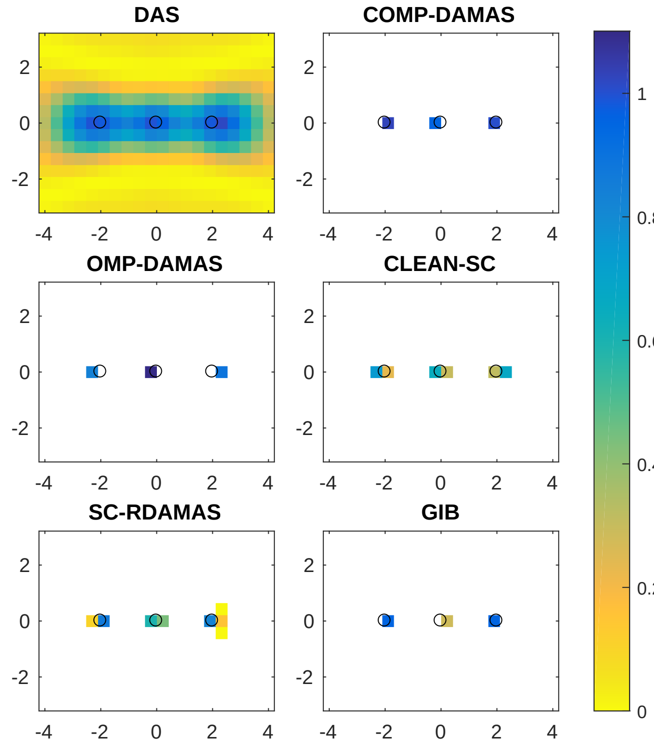

Fig. 1. Simulated results for scenario 1 with $f = 2$ kHz and no noise showing the delay-and-sum image (top left); as well as the deconvolved images from COMP-DAMAS (top right), OMP-DAMAS (middle left), CLEAN-SC (middle right), SC-RDAMAS (bottom left), and GIB (bottom right). The black circles indicate the actual sources positions. The unit on the axes is meter.

Table 1 demonstrates that the accuracy in terms of DOA of COMP-DAMAS is on par with SC-RDAMAS and GIB, and superior to OMP-DAMAS and CLEAN-SC. Table 2 shows that the reconstructed power accuracy of COMP-DAMAS is better than the other methods for high SNR, and about the same as OMP-DAMAS for lower SNR (and still better than CLEAN-SC, SC-RDAMAS and GIB). CLEAN-SC struggles with separating the two closely spaced sources in scenario 2, which leads to very inaccurate source power estimates.

Though the algorithm implementations have not been extensively optimized, it may still be instructive to compare the average runtimes on the simulated data. Since beamforming is common to all of the methods we have excluded it from the runtime comparison. Relative to OMP-DAMAS, which is the fastest of the four algorithms, the average runtime of COMP-DAMAS is about 2.5, about 160 for CLEAN-SC, about 800 for SC-RDAMAS, and about 1900 for GIB. Relative to the time needed for beamforming the difference between COMP-DAMAS and OMP-DAMAS is less than one tenth. For practical purposes, COMP-DAMAS is thus as fast as OMP-DAMAS, and more accurate.

Table 1. Average position error for simulated data [meter]

Scenario	SNR	COMP-DAMAS	OMP-DAMAS	CLEAN-SC	SC-RDAMAS	GIB
1	∞	0.14	0.28	0.28	0.14	0.14
1	0 dB	0.14	0.28	0.21	0.14	0.14
1	-6 dB	0.14	0.28	0.21	0.14	0.14
1	-9 dB	0.14	0.28	0.21	0.14	0.14
1	-12 dB	0.14	0.28	0.21	0.14	0.14
2	∞	0.10	0.17	$0.17^{\star}$	0.10	0.10
2	0 dB	0.10	0.17	$0.17^{\star}$	0.10	0.10
2	-6 dB	0.10	0.17	$0.17^{\star}$	0.10	0.10
2	-9 dB	0.10	0.24	$0.10^{\star}$	0.10	0.10
2	-12 dB	0.17	0.24	$0.17^{\star}$	0.10	0.10
3	∞	0.16	0.32	0.23	0.16	0.16
3	0 dB	0.16	0.32	0.23	0.20	0.16
3	-6 dB	0.16	0.32	0.29	0.20	$0.16^{\dagger}$
3	-9 dB	0.16	0.32	0.29	0.20	$0.21^{\dagger}$
3	-12 dB	0.16	0.36	0.29	0.20	$0.21^{\dagger}$

Table 2. Average relative power error for simulated data [%]

Scenario	SNR	COMP-DAMAS	OMP-DAMAS	CLEAN-SC	SC-RDAMAS	GIB
1	∞	3	12	31	24	27
1	0 dB	3	13	24	23	28
1	-6 dB	4	13	38	23	27
1	-9 dB	6	12	20	23	26
1	-12 dB	13	11	24	23	24
2	∞	4	7	$61^{\star}$	15	52
2	0 dB	3	6	$57^{\star}$	23	52
2	-6 dB	4	5	$58^{\star}$	24	49
2	-9 dB	7	11	$67^{\star}$	18	40
2	-12 dB	17	18	$67^{\star}$	25	36
3	∞	3	10	21	42	21
3	0 dB	3	8	20	44	21
3	-6 dB	7	4	20	41	$25^{\dagger}$
3	-9 dB	9	8	20	43	$25^{\dagger}$
3	-12 dB	20	23	21	39	$27^{\dagger}$

5. APPLICATION TO EXPERIMENTAL DATA

To test the proposed method and compare its accuracy with similar methods for solving the DAMAS inverse problem we have set up an experiment using two identical loudspeakers emitting uncorrelated white noise. We have applied COMP-DAMAS and the four other methods also used in section 4 to the DAS image for $f = 2.4$ kHz with 40×30 source points. We have used $K \in \{10, 100, 1000\}$ snapshots at 128 samples each to estimate the CSM. The DAS image along with the deconvolved images for $K = 1000$ are shown in fig. 2. We have used the same position error metric as in section 4 to evaluate the various methods, the results of which are summarized in table 3. As before, the dagger symbol signifies that the GIB method failed to locate the weakest source for $K \in \{10, 100\}$ and the listed number is only applicable to the strongest source. These results show that COMP-DAMAS is more accurate than the other methods in this experimental situation (except maybe CLEAN-SC at $K \geq 100$), and performs well even on few samples (10 snapshots of 128 samples at a sampling rate of 44.1 kHz corresponds to a sampling duration of 29 ms). We have not calculated the reconstructed source power error, since we did not have access to accurate measurements of the source power.

6. CONCLUSION

We have presented an acoustic deconvolution method for solving the DAMAS inverse problem, which we refer to as Clustered OMP-DAMAS (COMP-DAMAS). We have benchmarked its accuracy against four other algorithms: OMP-DAMAS [17], CLEAN-SC [6], SC-RDAMAS [12, 13], and GIB [10]. The presented algorithm has a higher overall accuracy in terms of direction-of-arrival and reconstructed source power over the range of simulated situations, as well as on real experimental data. The presented method is practically as fast as OMP-DAMAS on the simulated data, and substantially faster than CLEAN-SC, SC-RDAMAS and GIB.

The performance of COMP-DAMAS depends on choosing a value of the regularization parameter λ that is appropriate for the given imaging grid density. Future work on this method should therefore seek to find an automatic method for regularization. Another potential improvement is in the way that the final source powers are synthesized from the expansion coefficients from stage 1. Rather than heuristic clustering and local optimization within each cluster, improvements might be obtained by using statistical and/or information-theoretical criteria to determine a globally optimal model of point sources.

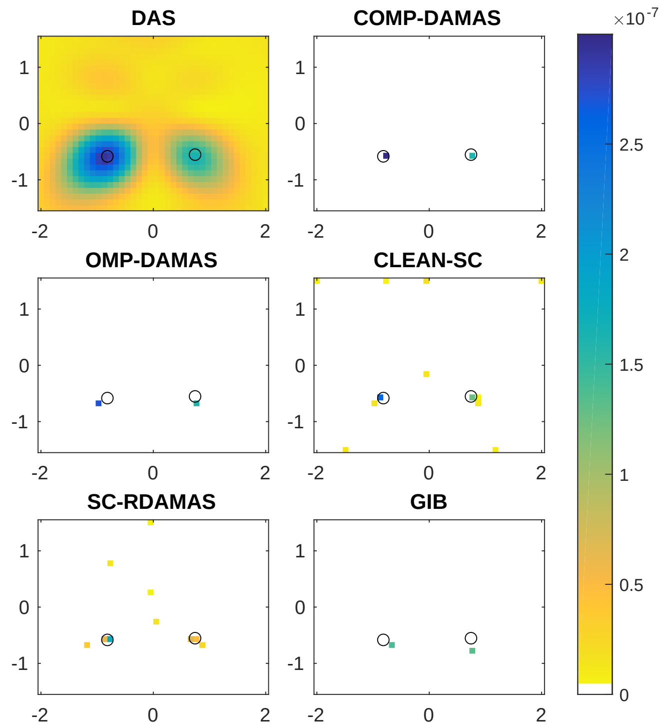

Fig. 2. Experimental results showing the delay-and-sum image for $f = 2.4$ kHz and $K = 1000$ (top left); as well as the deconvolved images from COMP-DAMAS (top right), OMP-DAMAS (middle left), CLEAN-SC (middle right), SC-RDAMAS (bottom left), and GIB (bottom right). The black circles indicate the actual source positions. The unit on the axes is meter.

Table 3. Average position error for experimental data [meter]

K	COMP-DAMAS	OMP-DAMAS	CLEAN-SC	SC-RDAMAS	GIB
10	0.03	0.13	0.10	0.07	$0.28^{\dagger}$
100	0.07	0.15	0.04	0.07	$0.08^{\dagger}$
1000	0.03	0.15	0.04	0.07	0.18

7. REFERENCES

[1] Thomas F. Brooks and William M. Humphreys, "A deconvolution approach for the mapping of acoustic sources (DAMAS) determined from phased microphone arrays," *Journal of Sound and Vibration*, vol. 294, no. 4, pp. 856–879, 2006.

[2] Robert Dougherty, "Extensions of DAMAS and Benefits and Limitations of Deconvolution in Beamforming," in *11th AIAA/CEAS Aeroacoustics Conference*. 2005, American Institute of Aeronautics and Astronautics.

[3] Zhigang Chu and Yang Yang, "Comparison of deconvolution methods for the visualization of acoustic sources based on cross-spectral imaging function beamforming," *Mechanical Systems and Signal Processing*, vol. 48, no. 12, pp. 404–422, Oct. 2014.

[4] U. J. Schwarz, "Mathematical-statistical Description of the Iterative Beam Removing Technique (Method CLEAN)," *Astron. Astrophys*, vol. 65, pp. 345–356, 1978.

[5] Yanwei Wang, Jian Li, Petre Stoica, Mark Sheplak, and Toshikazu Nishida, "Wideband RELAX and wideband CLEAN for aeroacoustic imaging," *The Journal of the Acoustical Society of America*, vol. 115, no. 2, pp. 757–767, Feb. 2004.

[6] Pieter Sijtsma, "CLEAN Based on Spatial Source Coherence," *International Journal of Aeroacoustics*, vol. 6, no. 4, pp. 357–374, Dec. 2007.

[7] Tarik Yardibi, Jian Li, Petre Stoica, and Louis N. Cattafesta Iii, "Sparsity constrained deconvolution approaches for acoustic source mapping," *The Journal of the Acoustical Society of America*, vol. 123, no. 5, pp. 2631–2642, May 2008.

[8] Robert Tibshirani, "Regression Shrinkage and Selection via the Lasso," *Journal of the Royal Statistical Society. Series B (Methodological)*, vol. 58, no. 1, pp. 267–288, 1996.

[9] Ennes Sarradj, "A fast signal subspace approach for the determination of absolute levels from phased microphone array measurements," *Journal of Sound and Vibration*, vol. 329, no. 9, pp. 1553–1569, Apr. 2010.

[10] Takao Suzuki, "L1 generalized inverse beam-forming algorithm resolving coherent/incoherent, distributed and multipole sources," *Journal of Sound and Vibration*, vol. 330, no. 24, pp. 5835–5851, Nov. 2011.

[11] Siyang Zhong, Qingkai Wei, and Xun Huang, "Compressive sensing beamforming based on covariance for acoustic imaging with noisy measurements," *The Journal of the Acoustical Society of America*, vol. 134, no. 5, pp. EL445–EL451, Nov. 2013.

[12] Ning Chu, Ali Mohammad-Djafari, and Jos Picheral, "Robust Bayesian super-resolution approach via sparsity enforcing a priori for near-field aeroacoustic source imaging," *Journal of Sound and Vibration*, vol. 332, no. 18, pp. 4369–4389, 2013.

[13] Ning Chu, Jos Picheral, Ali Mohammad-djafari, and Nicolas Gac, "A robust super-resolution approach with sparsity constraint in acoustic imaging," *Applied Acoustics*, vol. 76, pp. 197–208, Feb. 2014.

[14] J. Joseph, N. S. Kumar, R. D. M, and K. K. K. P, "CS Based Acoustic Source Localization and Sparse Reconstruction Using Greedy Algorithms," in *2015 Fifth International Conference on Advances in Computing and Communications (ICACC)*, Sept. 2015, pp. 403–407.

[15] Wenyi Wang and Renbiao Wu, "High Resolution Direction of Arrival (DOA) Estimation Based on Improved Orthogonal Matching Pursuit (OMP) Algorithm by Iterative Local Searching," *Sensors (Basel)*, vol. 13, no. 9, pp. 11167–11183, Aug. 2013.

[16] Y. C. Pati, R. Rezaiifar, and P. S. Krishnaprasad, "Orthogonal matching pursuit: recursive function approximation with applications to wavelet decomposition," in *1993 Conference Record of The Twenty-Seventh Asilomar Conference on Signals, Systems and Computers, 1993*, Nov. 1993, pp. 40–44 vol.1.

[17] Thomas Padois and Alain Berry, "Orthogonal matching pursuit applied to the deconvolution approach for the mapping of acoustic sources inverse problem," *The Journal of the Acoustical Society of America*, vol. 138, no. 6, pp. 3678–3685, Dec. 2015.

[18] Walid Osamy, Ahmed Salim, and Ahmed Aziz, "Sparse Signals Reconstruction via Adaptive Iterative Greedy Algorithm," *International Journal of Computer Applications*, vol. 90, no. 17, pp. 5–11, Mar. 2014.